

Torque vectoring for improving stability of small electric vehicles

W Grzeżożek¹ and K Weigel-Milleret¹

¹ Institute of motor Vehicles and Internal Combustion Engines, Cracow University of Technology, Al. Jana Pawla II 37, 31-864 Krakow, Poland

E-mail: witek@mech.pk.edu.pl, krzysztof.weigel-milleret@mech.pk.edu.pl

Abstract. The electric vehicles solutions based on the individually controlled electric motors propel a single wheel allow to improve the dynamic properties of the vehicle by varying the distribution of the driving torque. Most of the literature refer to the vehicles with a track typical for passenger cars. This paper examines whether the narrow vehicle (with a very small track) torque vectoring bring a noticeable change of the understeer characteristics and whether torque vectoring is possible to use in securing a narrow vehicle from roll over (roll mitigation). The paper contains road tests of the steering characteristics (steady state understeer characteristic quasi-static acceleration with a fixed steering wheel ($\delta H = \text{const}$) and on the constant radius track ($R = \text{const}$)) of the narrow vehicle. The vehicle understeer characteristic as a function of a power distribution is presented.

1. Introduction

Modern microcars often use electric motors to drive. That design reduces costs of driving and the negative impact of the vehicle on the environment. Common in European cities is setting a special zones with limited or total ban entry of cars equipped with combustion engines (zero emission zone), where electric vehicles can freely drive. Often the legal system is favouring microcars in relation to full size vehicles (often by lower taxes and lower insurance rates). Driver's license category AM, B1 or ID is usually sufficient to drive these vehicles. Design intent of microcars can be summarized in the following points:

1. Small size of the vehicle (length not exceeding 3 m), the body that protect against precipitation
2. Interior space should be enough for one person and a small luggage
3. Electric drive
4. The minimum range of approx. 60 km
5. Approval in L6e category (AM driver's license) or L7e (B1 driver's license)
6. Low price
7. Good maneuverability

A prototype vehicle MIST (acronym created from the first letters expressing Individual Urban Vehicle) was designed and made at the Cracow University of Technology (shown in Figure 1). MIST body is made as a welded space frame with a mounting points of the suspension. This design provides high rigidity in three axes, and high torsional rigidity of the body. Body has bilateral access to the interior



and has enough space for the driver and a small luggage. Good visibility to the front and to the sides has been achieved by the large windscreen and thin front posts.



Figure 1. MIST microcar.

The front suspension of the vehicle is doubled pushed arm. The small wheelbase has allowed usage of a dependent suspension of the front wheels. Suspension movements cause the parallel movement of the front wheels. This solution increased the roll stiffness of the vehicle.

The rear suspension is semi-independent twist beam with towed arms. Semi-independent suspension solution for the rear suspension ensures high roll stiffness of the vehicle. Traction batteries container is set between rear suspension arms.

The car uses two brushless AC motors installed in the rear wheels of the vehicle to drive. An active control of the electric drive allows a regulation of the distribution of the driving torque. Hydraulic disc brakes mounted on all wheels of the vehicle.

2. Torque vectoring

The first generation of electric vehicles were build by replacing the internal combustion engine with an electric motor while keeping the same construction of the powertrain. The electric motor were positioned at the main gear of the differential. Current solutions based on the individually controlled electric motors propel a single wheel allow to improve the dynamic properties of the vehicle by varying the distribution of the driving torque (and braking torque) [3].

2.1. Steady-state torque vectoring

In order to measure a vehicle steering the gradient of steering wheel angle related to the lateral acceleration, normalized by steering system transmission ratio has been adopted. It is called the gradient of understeer, which is defined as [7]:

$$Grad_p = \frac{\partial \delta_H}{\partial a_y} \frac{1}{i_s} - \frac{\partial \delta_D}{\partial a_y} \tag{1}$$

where:

- δ_H - steering wheel angle,
- i_s - steering transmission ratio,
- δ_D - comparative, dynamic steering wheel angle,
- a_y - lateral acceleration.

$$\delta_D = \frac{L}{R} \tag{2}$$

- L- wheelbase,
- R- track radius of the center of mass

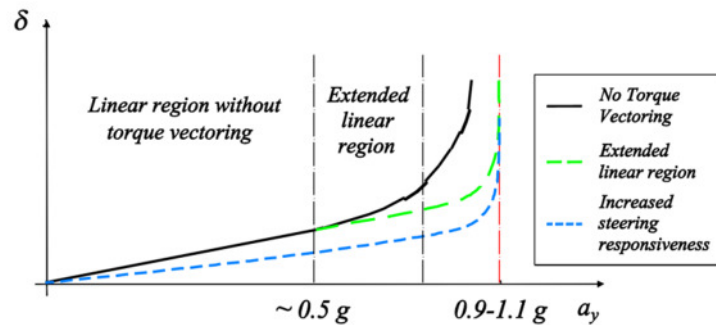


Figure 2. Modifications of the understeer characteristic achievable by torque vectoring [2].

Vehicle steering characteristic can be represented as the steering wheel angle as a function of the vehicle lateral acceleration (Figure 2). The trend of lateral acceleration at understeer vehicles is normally linear up to certain value of lateral acceleration (usually approx. 0.5g) and then increases non-linearly to a maximum value. It is the maximum possible lateral acceleration to obtain in a steady state cornering. A scientific literature describes the theoretical and experimental evidence that the torque vectoring can lead to extending the linear response of the vehicle to the steering signal, increasing the maximum lateral acceleration and changing the understeer gradient [1,4,6].

2.2. Transient state torque vectoring

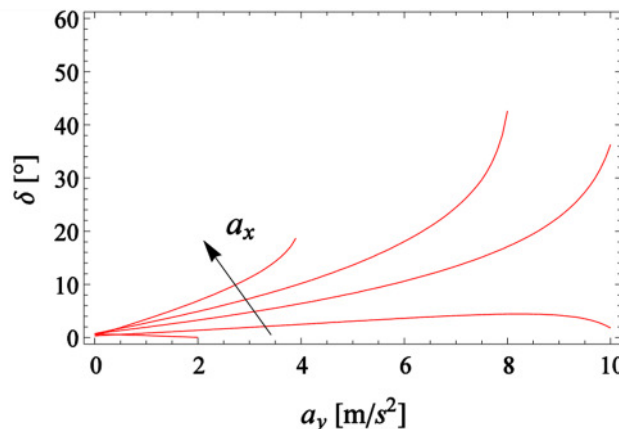


Figure 3. Vehicle understeer characteristic, steering wheel angle as a function of the lateral acceleration.

In the transient state vehicle understeer characteristic is a function of a longitudinal acceleration of the vehicle, which is highlighted in Figure 3. The increasing of the longitudinal acceleration reduces the linear response region of the vehicle to the steering signal. To improve the vehicle performance at the transient state two different torque vectoring strategies can be implemented: i) driving torque proportional to the each wheel normal (vertical) load (see Figure 4.); ii) driving torque distribution allowing achieving the same longitudinal slip ratio on each wheel of the vehicle [6]. Both strategies allow to reduce the understeer gradient difference and expand the linear respond region .

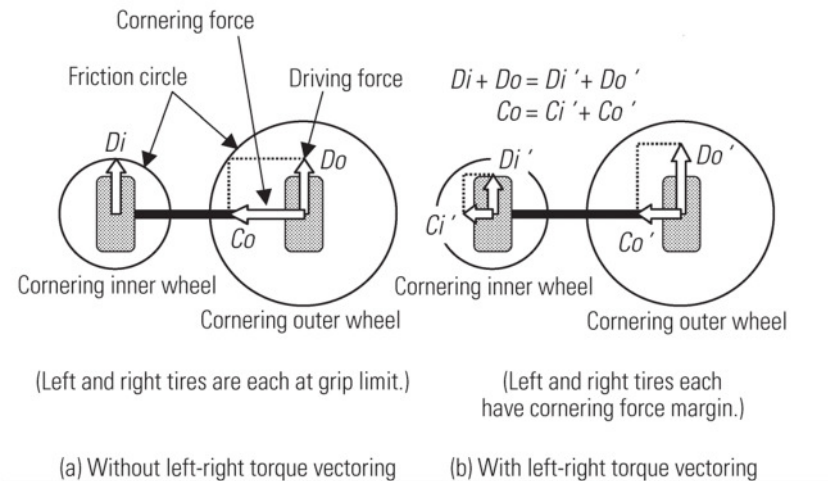


Figure 4. Driving force proportional to the friction force (b); where:
 i subscript - inside motor, o subscript - outside motor [5].

Torque vectoring reduces the vehicle power consumption while cornering. Simulations carried out by [2] point to a few percent reduction of the vehicle energy consumption in relation to the vehicle with the same parameters without differentiation of torque. This result shows that the torque vectoring strategies not only increases the vehicle dynamic performance, but also optimizes the usage of the battery energy.

3. Test

Most of the extensive body of literature refer to the vehicles with a track typical for passenger cars. This paper examines whether the narrow vehicle (with a very small track) torque vectoring bring a noticeable change of the understeer characteristics and whether torque vectoring is possible to use in securing a narrow vehicle from roll over (roll mitigation). The tests was conducted for a 0.7m track microcar.

3.1. Performed tests:

- acceleration and top speed test,
- steady state understeer characteristic quasi-static acceleration with a fixed steering wheel ($\delta H = \text{const}$) and on the constant radius track ($R = \text{const}$).



Figure 5. MIST microcar equipped with measuring set.

V-box equipment was used for measuring the speed and position of the vehicle in a fixed external coordinate system. V-box is a device for measuring the coordinates of a point associated with the vehicle, which calculate the speed, driving distance and the yaw rate, roll rate and a pitch rate. The V-box measurement is based on satellite navigation (GPS and GLONASS). Measure data are recorded on the internal memory card (Compact Flash). Furthermore, the electric motors currents were recorded. MIST equipped with measuring set is shown in Figure 5.

3.2. Steering characteristic

Tests with a constant steering angle to the left have been carried out ($\Delta H = \text{const}$). The steering wheel has been blocked at 24° turn. Three different power distribution have been performed: i) power only to the inside wheel motor; ii) power only to the outside wheel motor; iii) constant torque split between the wheels 50%: 50%. Quasi-static acceleration from standstill start to achieve the maximum lateral acceleration or safety limit due to the possibility of rollover. The evaluation of the vehicle cornering performance has been accomplished through the analysis of the trend of the steering angle increment as a function of the lateral acceleration. The steering angle increment is defined as (see Figure 6):

$$\delta_0 - \alpha_1 + \alpha_2 = \frac{L}{R} \quad (3)$$

$$\alpha_2 - \alpha_1 = \frac{L}{R} - \frac{L}{R_0} = \frac{L}{R_0} \left(1 - \frac{R_0}{R}\right) = \delta_0 \left(1 - \frac{R_0}{R}\right) \quad (4)$$

$$\Delta\delta = \delta_0 \left(1 - \frac{R_0}{R}\right) \quad (5)$$

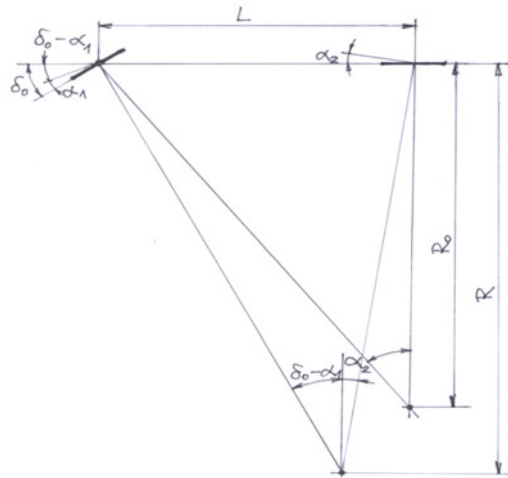


Figure 6. Constant steering wheel angle test [A Kleczkowski].

The constant radius of track $R = 17\text{m}$ tests have been performed (turning left). Three different power distribution have been performed: i) power only to the inside wheel motor; ii) power only to the outside wheel motor; iii) constant torque split between the wheels 50%: 50%. Quasi-static acceleration from standstill start to achieve the maximum lateral acceleration or the maximum speed at which the vehicle can be maintained on the track.

4. Test result

4.1. Acceleration and top speed

The top speed of 41 km/h has been reached. This was due to a too short test track (interruption of measurement after reaching the end of the track). It differs only slightly from the top speed calculated on the data obtained from the motors manufacturer. Average acceleration in the range 0 - 25 km/h was 1 m/s^2 , and in the range 0 - 40 km/h was 0.7 m/s^2 (see Figure 7).

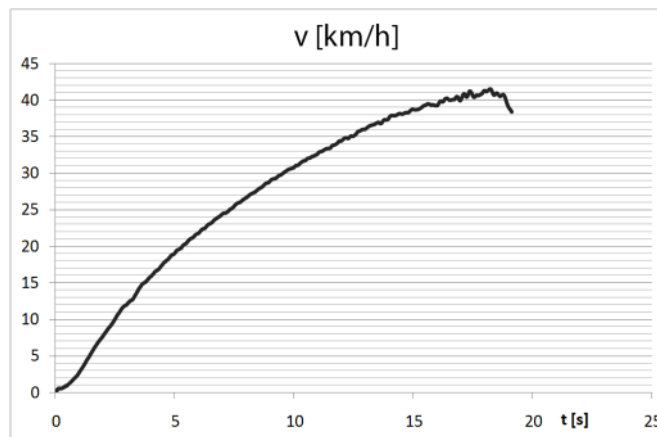


Figure 7. Speed as a function of the time during the top speed test.

4.2. Constant steering wheel angle test

The trend of the steering angle increment is dependent on the torque distribution. Supplying the power to the inside motor causes achieving the smallest linear response region and the largest understeer gradient in the non-linear region (Figure 8). The equal distribution of drive torque causes the whole tested lateral acceleration region $0 < a_y < 4\text{m/s}^2$ were almost linear response region which understeer

gradient approximately $\text{grad} = 0$ (Figure 9). Supplying the power to the outside motor causes the oversteer vehicle behaviour (understeer gradient < 0) (Figure 10). The power distribution impact on the steering angle increment is shown in Figure 11.

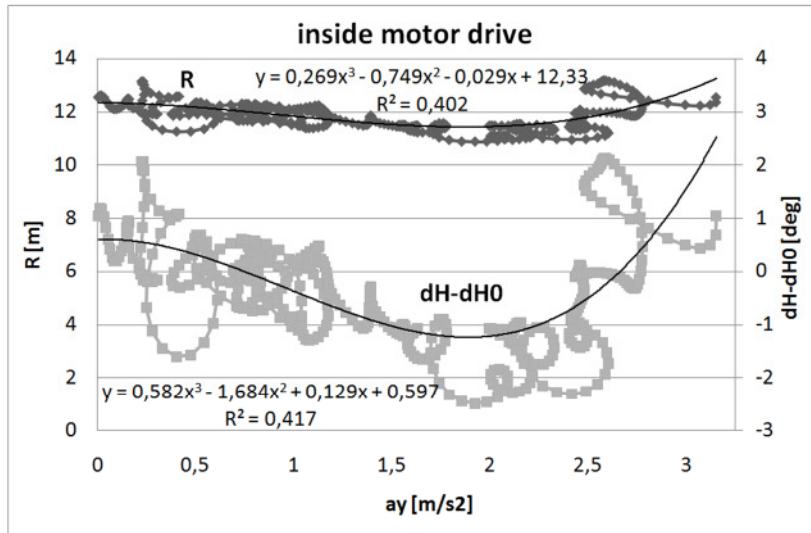


Figure 8. Radius of turn [m](black) and steering angle increment [deg](grey) as a function of lateral acceleration [m/s²] during constant steering wheel angle test - inside motor drive.

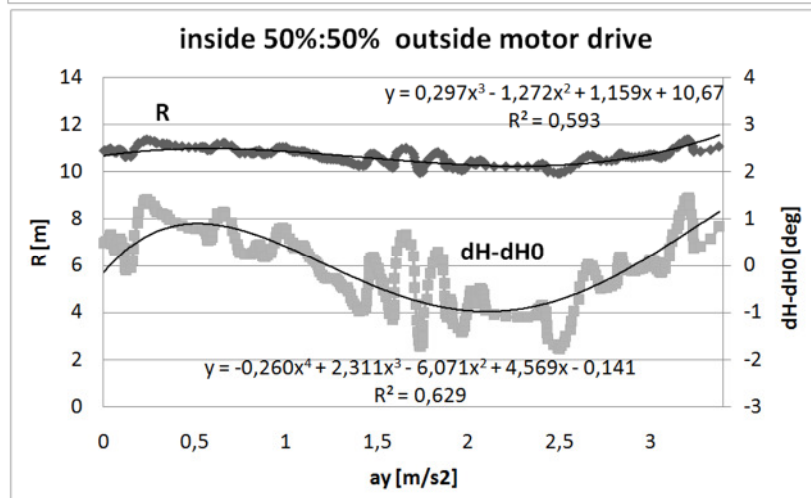


Figure 9. Radius of turn [m](black) and steering angle increment [deg](grey) as a function of lateral acceleration [m/s²] during constant steering wheel angle test - equal power distribution.

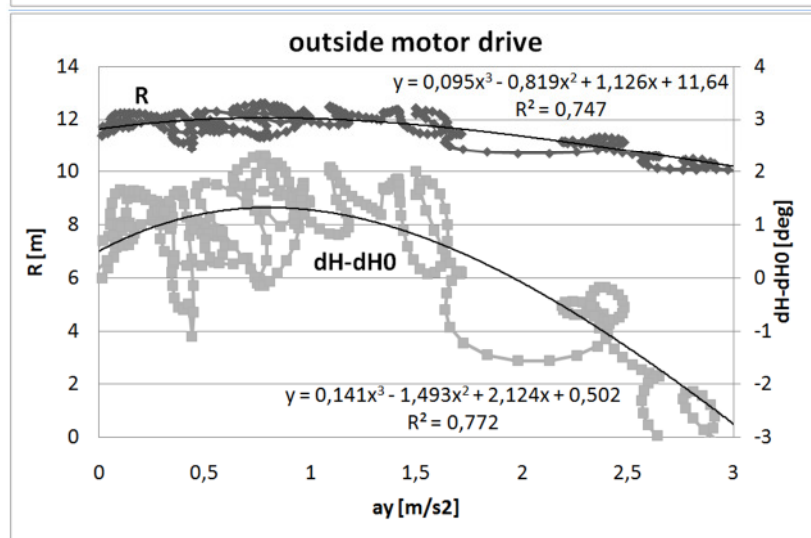


Figure 10. Radius of turn [m](black) and steering angle increment [deg](grey) as a function of lateral acceleration [m/s²] during constant steering wheel angle test - outside motor drive.

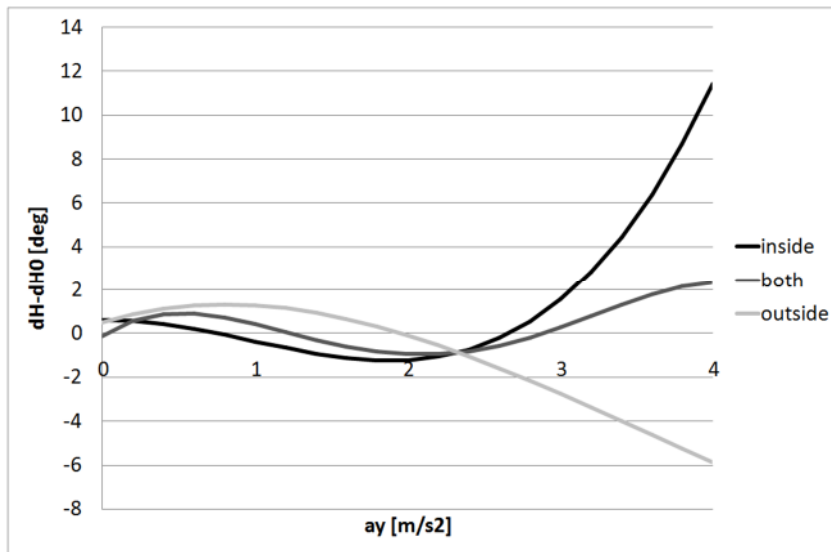


Figure 11. Steering angle increment [deg]: inside motor drive (black), both motor drive (dark grey), outside motor drive (light grey) as a function of lateral acceleration [m/s²] during constant steering wheel angle test.

4.3. Constant radius of track test

The evaluation of the vehicle cornering performance for the constant radius of track has been accomplished through the analysis of the trend of the steering angle as a function of the lateral acceleration. Supplying the power to the inside motor or equal distribution of drive torque causes understeer behaviour of the microcar (see Figure 12 and Figure 13). Supplying the power to the inside motor raises the understeer gradient. Supplying the power to the outside motor causes oversteer behaviour (see Figure 14). The understeer gradient is below 0. During the test increasing the lateral acceleration has caused decreasing the steering wheel angle.

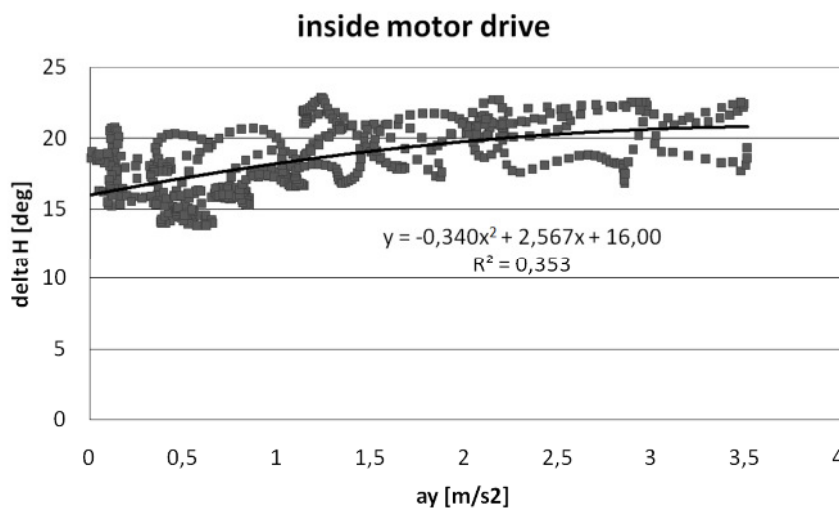


Figure 12. Steering wheel angle [deg]: as a function of lateral acceleration [m/s²] during constant radius of track test - inside motor drive.

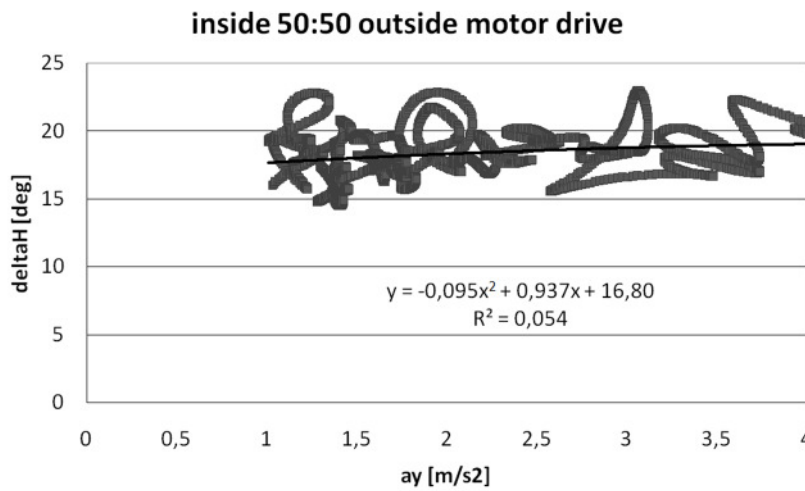


Figure 13. Steering wheel angle [deg]: as a function of lateral acceleration [m/s²] during constant radius of track test - equal power distribution.

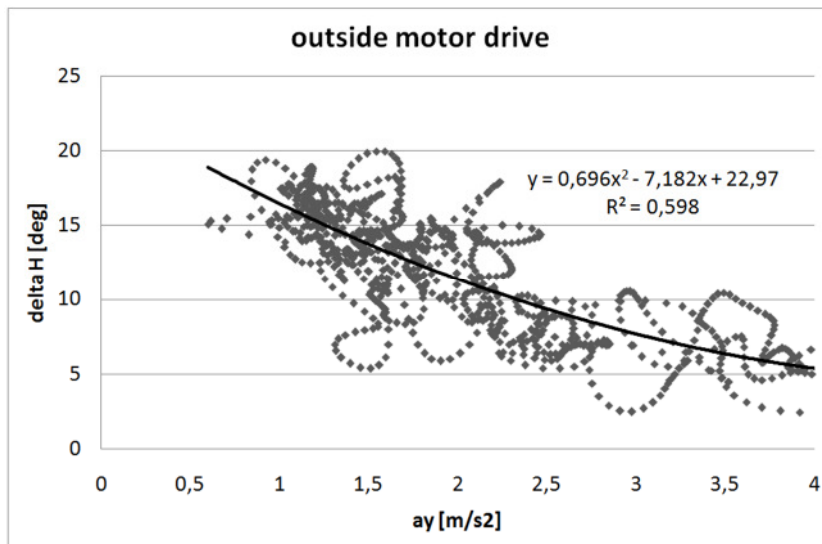


Figure 14. Steering wheel angle [deg]: as a function of lateral acceleration [m/s²] during constant radius of track test - outside motor drive.

5. Conclusion

Performed test shows that the torque vectoring can significantly affects the stability characteristics of the narrow car. A wide range of differences from understeer to oversteer and the experience gained in carrying out the tests (the detachment of two wheels from the road surface) suggests that it is possible and desirable to build a roll mitigation system based on the drive torque vectoring. Its operation is limited to acceleration of the vehicle or driving at a constant speed (with partial and full throttle). The undoubted advantage is, however, no energy losses when working, in contrast to systems based on the ESP to stabilize the vehicle's in which vehicle brakes are used. This is an advantage especially in electric vehicles. The density of energy stored in the traction batteries is many times lower than the density of energy in gasoline or diesel fuel stored in an internal combustion engine powered vehicle tank, and any energy loss dissipated in brakes significantly reduces the range of the vehicle.

References

- [1] Abe M 1986 A theoretical analysis on vehicle cornering behaviors in acceleration and braking; *Vehicle System Dynamics*, **15**
- [2] De Novellis L, Sorniotti A, Gruber P, Shead L, Ivanov V and Hoepfing K 2012 Torque vectoring for electric vehicles with individually controlled motors: State-of-the-art and future developments; *26th International Electric Vehicle Symposium (EVS26)*

- [3] Meier T, Rinderknecht S and Fietzek R 2011 Electric power train configurations with appropriate transmission systems; *SAE Technical Paper 2011-01-0942*
- [4] Shibahata Y, Shimada K and Tomari T 1993 Improvement of vehicle maneuverability by direct yaw moment control, *Vehicle System Dynamics*, **22**; 465-81
- [5] Sawase K, Ushiroda Y and Miura T 2006 Left-Right torque vectoring technology as the core of super all wheel control (S-AWC); *Mitsubishi Motors Technical Review*, **18**; 16-23
- [6] Shimada K and Shibahata Y 1994 Comparison of three active chassis control methods for stabilizing yaw moments; *SAE Technical Paper*, **940870**; 87-97
- [7] Winkler C, Aurell J 1998 Analysis and testing of the steady-state turning of multiaxle trucks; *Heavy Vehicle Weights and Dimensions, 5th international symposium*; 135-61